Articles

Silicon-29 Magic-Angle Spinning Nuclear Magnetic Resonance Spectroscopy of Sintered Silicon Nitride Ceramics

Keith R. Carduner,* R. O. Carter III, M. J. Rokosz, C. Peters, G. M. Crosbie, and E. D. Stiles

Ford Motor Company, Research Staff, Dearborn, Michigan 48121

Received October 11, 1988

Silicon-29 magic-angle spinning (MAS) nuclear magnetic resonance (NMR) spectroscopy is used to study the grain boundary phases that result during sintering of Si_3N_4 powders in the presence of yttria and alumina added as sintering aids. A series of five Si_3N_4 ceramic cylinders are examined. The densification of α- to β-Si_3N_4 is clearly observed, and α/β ratios are determined by an NMR spectral subtraction/integration procedure when incomplete conversion occurs. Y–Si–O–N phases resulting from the reaction of Y_2O_3 with the α-Si_3N_4 during high-temperature sintering are observed by the ^{29}Si MAS NMR technique. When compared with quantitative powder X-ray diffraction analysis of the same samples, differences in composition are observed in the sintered ceramic components that may be explained by the presence of amorphous phases as well as paramagnetic impurities. The comparison of techniques points out the range of applicability of each analytical approach and suggests that the best way to quantify grain boundary phases in sintered Si_3N_4 ceramic requires a multiple technique approach.

Introduction

Solid-state ^{29}Si magic-angle spinning (MAS) nuclear magnetic resonance (NMR) previously has been used to provide quantitative information regarding the morphology of silicon nitride (Si_3N_4) powders and to analyze, qualitatively and quantitatively, for silicon-containing impurities.[1] The development of the MAS NMR analytical technique was initiated by the growing need for accurate quantitative information regarding the phase composition of Si_3N_4 powders, precursors to sintered ceramic components.[1] The phase composition of Si_3N_4 powders has been shown to influence processing into structural ceramics,[2,3] materials that are finding increasing application in the transportation industry.[4] The three types of Si_3N_4—the crystalline α and β phases and amorphous Si_3N_4 material—each have characteristic ^{29}Si MAS NMR resonance bands.[1] A Si_3N_4 ^{29}Si MAS NMR resonance from a given powder sample can be analyzed as the superposition of these three characteristic line shapes. This assumption led to quantitative analysis of the weight percent of each polytype from a series of nominally α-phase samples. Additionally, it was found that the distinct chemical shifts of silicates, elemental silicon, and silicon oxynitride allows for the quantitative analysis of these species from the ^{29}Si MAS NMR spectrum. The analyses of seven different α-phase powders, four of commercial origin and three experimental powders, were compared with the results from powder X-ray diffraction analysis.[1] This comparison demonstrated that the NMR technique is sensitive to a different composition than that observed with X-ray diffraction. This difference was ascribed to the ability of the NMR technique to also count nuclei in amorphous or noncrystalline environments.

Building on that work, this report demonstrates the application of ^{29}Si MAS NMR to the qualitative and quantitative analysis of sintered Si_3N_4 ceramics. The application of ^{27}Al MAS NMR to this material is also introduced. The densification of α-Si_3N_4 powder into an interlocking structure of β-Si_3N_4 needles occurs by a high-temperature liquid-phase sintering mechanism aided by the addition of small amounts of sintering aids.[5] In this process, the precursor powder is heated or hot pressed in the absence of oxygen.[6] During sintering, the additives react with a small amount of the Si_3N_4 to form new compounds at trace levels that reside at the grain boundaries between the needles of β-Si_3N_4. The location of sintering phases at grain boundaries has been demonstrated, most conclusively, by results from electron microscopy.[7] The specific sintering additive package examined here is a combination of yttria, Y_2O_3, and alumina, Al_2O_3. Yttria is typically added in to the level of 5–10% by weight,[8] while the alumina is at a somewhat lower level, normally around 1–2.5%.

The reported phase diagram of the Y–Si–O–N system contains four Y–Si–O–N species, three with Y–Si–N, and two Y–Si–O compounds.[9] The NMR spectra for some of these materials have been reported.[10] With these data and spectra of similar samples identified by using X-ray diffraction, the analysis of the bulk and of the trace compo-

(1) Carduner, K. R.; Carter III, R. O.; Milberg, M. E.; Crosbie, G. M. *Anal. Chem.* **1987**, *59*, 2794.
(2) Engel, W. *Powder Metall. Int.* **1987**, *10*, 124.
(3) Woettig, G.; Ziegler, G. *Powder Metall. Int.* **1986**, *18*, 25.
(4) Kalamasz, T. G.; Goth, G.; Worthen, R. P.; Pasto, A. E. *Automot. Eng.* **1988**, *96*, 64.
(5) Greskovich, C.; Prochazka, S. *Ceramic Microstructure 1986*; Pask, J. A., Evans, A. G., Eds.; Plenum Press: New York, 1987; p 35.
(6) Milberg, M. E. *CHEMTECH* **1987**, *17*, 552.
(7) Thomas, G. *Ceramic Microstructure 1986*; Pask, J. A., Evans, A. G., Eds.; Plenum Press; New York, 1987; p 55.
(8) Gazza, G. E. *Bull. Am. Ceram. Soc.* **1975**, *54*, 778.
(9) Thompson, D. P. *Tailoring Multiphase and Composite Ceramics*; Tressler, R. E., Messing, G. L., Pantano, C. G., Newnham, R. G., Eds.; Plenum: New York, 1986; pp 79–91.
(10) Dupree, R.; Lewis, M. H.; Smith, M. E. *J. Am. Chem. Soc.* **1988**, *110*, 1083.

0897-4756/89/2801-0302$01.50/0

sition for five systematically prepared sintered Si_3N_4 ceramic cylinders is reported. The X-ray diffraction analysis of these materials is also reported, and it will be seen that, as was reported for the powders,[1] significant difference exists between the analytical results from the two techniques. These differences are attributed to two effects: (1) the inability of the X-ray technique to observe domains that are extremely small (smaller than 100 Å) or regions that are noncrystalline; (2) on the other hand, the exclusion from the NMR spectrum of components that are rapidly relaxed by the presence of paramagnetic impurities. The intergranular Y–Si–O–N phases have important consequences on physical and thermal properties of Si_3N_4 components. In particular, different crystalline or amorphous grain boundary phases have different thermal expansion and oxidation susceptibilities. This variability strongly affects high-temperature ceramic performance. Also, well-crystallized intergranular phases prevent high-temperature plastic deformation. Thus, techniques for their accurate identification and quantitation of grain boundary phases can provide an important tool for studies into the control of microstructure for improved ceramic performance.[6,11]

In this report, it is shown that as with the Si_3N_4 powders, ^{29}Si MAS NMR spectroscopy can often be applied to detect, identify, and quantify the Y–Si–O–N grain boundary phases. In the following, there will also be some discussion of the types of phases that appear to form during sintering along with multinuclear spectra demonstrating their detection in sintered ceramic.

Experimental Section

Samples. Five samples (and repeats) of sintered Si_3N_4 ceramics were prepared as described elsewhere.[12] These samples were part of a designed study of a pressureless sintering program for optimum mechanical and physical properties. In a five-step sintering cycle (ramp to intermediate temperature, hold at intermediate temperature, ramp to highest temperature, hold at higher temperature, and ramp back to room temperature), the effects of two different levels in three of the steps were considered. The factors considered were the intermediate hold temperature, ramp rate to 1800 °C (the highest temperature), and then hold time at 1800 °C. The effect of changes in these factors on final density, morphology, and mechanical properties are presented in ref 12. All samples contained 10 wt % Y_2O_3 and 2.25 wt % Al_2O_3 and used UBE E-10 (see ref 1) Si_3N_4 powder.

Six samples of mixed Y–Si–O–N phases were also acquired from a study of these materials whose goal was categorization of their powder X-ray diffraction patterns. These materials had been prepared by using techniques similar to those of Dupree et al.[10] These samples were not pure examples of the different possible Y–Si–O–N phases but were still useful for identifying the characteristic ^{29}Si resonance frequencies by ^{29}Si MAS NMR spectroscopy. A sample of β'-sialon Si_5AlON_7 was provided by M. E. Smith of the University of Warwick.

Quantitative X-ray Diffraction. Powder samples were prepared by crushing pieces of the sintered ceramic, remnants of the NMR sample preparation, in a steel impact mortar to a particle size of 45 μm or less. Repeated sieve separation and crushing cycles ensured a powder composition representative of the bulk material. In one instance, the actual NMR sample was crushed and analyzed. The powder was loaded into flat sample holders and leveled with a knife edge for data collection.

An automated X-ray powder diffractometer equipped with a diffracted beam graphite monochromator and scintillation detector was used to collect digital θ–2θ step-scanned spectra in the range $16.0° < 2\theta < 37°$, $2\theta = 0.025°$, $t = 5.0$ s (Cu Kα X-rays). Lorentzian peak parameters, including centroid ($2\theta_{ci}$) and area (A_i), for i = 1–16 possible peaks, were calculated by using a standard fitting routine.

Four crystalline phases were considered in the quantitative fitting procedure: α-Si_3N_4,[13] β-Si_3N_4,[14] $YSiO_2N$,[15] and $Y_5(SiO_4)_3N$.[16] For these phases, the relative contributions to each peak area were calculated by using the known structural information including the crystal system, space group, unit cell dimensions, and the atomic coordinates given in ref 13–16. The resulting set of linear equations, $C_{ji}x_j = A_i$, was solved for the relative phases x_j such that $\sum x_j = 1$. Any microabsorption or extinction effects were ignored. This procedure is adequate for quantitative diffraction analysis of mixtures containing phase concentrations in a limited range.[17] In addition, prepared binary mixtures of Si_3N_4 powder and the yttria phases were also analyzed and produced satisfactory results using the same set of equations. Complete details are reported elsewhere.[18] The XRD and NMR results are compared in Table III (discussed below).

Spectroscopy. Solid-state ^{29}Si NMR spectra were acquired under MAS conditions at ambient temperature by using a Bruker MSL 300 spectrometer (^{29}Si resonance frequency of 59.5 MHz) and a Bruker MAS probe. Filling of the alumina MAS rotor required $^1/_2$ g of powder, when powders were studied, or ceramic cylinders weighing ca. 0.8 g. MAS speeds were typically 4 kHz. Two pulse sequences were employed. The first sequence was a single-read pulse (tip angle 75°) followed by acquisition and relaxation recycle delay. The second was a multiple-pulse saturation method for measurement of the spin–lattice relaxation time, T_1, a sequence appropriate for measurement of long T_1's.[19] All free induction decays were subjected to standard Fourier transformation and phasing. Initially, the chemical shifts were referenced to tetramethylsilane (TMS), whose resonance was periodically checked by inserting a MAS rotor full of liquid. Later, a solid-state reference was employed, sodium hexafluorosilicate (Na_2SiF_6), whose resonance was measured as −189.2 ppm with respect to TMS. Lack of discernible magnet drift over days suggests that the shifts are correct to at least ±0.1 ppm. Negative shifts represent more shielded environments.

The determination of the relative concentration of different silicon species must take into account differences in T_1. A rather wide dispersion of values was noted in the previous study of powders:[1] 43 ± 2 min for Si_3N_4, 3 ± 0.5 min for elemental silicon, and 40 ± 3 min for SiO_2 (sample of glass wool). For the mixed Y–Si–O–N phases, values of T_1 are comparable. Normally, a wait of 5 times the longest T_1 is required between repetitions of the experiment. In the present case, this would require 200 min. Instead, use of a 75° read pulse requires only a 1-h wait since this tip angle destroys only 74% of the initial magnetization, the amount relaxed in 1 h (assuming exponential relaxation). The price paid for the opportunity to repeat the experiment more than three times faster is a reduction of the NMR signal to 97% of its potential value after a 90° pulse on a fully relaxed system—a loss of only 3%. For all the ^{29}Si MAS spectra reported below, this program was employed.

Solid-state ^{27}Al MAS NMR spectra were acquired at 78.206 MHz by using a Bruker MAS probe that was specially made to be free of aluminum background signal. MAS rotors were ZrO_2 (these were also checked for background signal). A 4-kHz spinning speed was used for all spectra, and spinning was exclusively at the magic angle of 54.44°. Data were acquired as a free induction decay (FID) following preparation of transverse magnetization using a new pulse sequence recently presented.[20] This sequence increases resolution of ^{27}Al spectra in the solid state. Following acquisition, the FID was multiplied by a decaying exponential to reduce noise and then processed into a frequency-domain

(11) Lange, F. F.; Singhal, S. C.; Kuznicki, R. C. *J. Am. Ceram. Soc.* **1977**, *60*, 249.
(12) Crosbie, G. M.; Nicholson, J. M.; Stiles, E. D. *Bull. Am. Ceram. Soc.* **1989**, June.
(13) Ruddelsden, S. N.; Pepper, P. *Acta Crystallogr.* **1958**, *11*, 405.
(14) Hardie, D.; Jack, K. H. *Nature* **1957**, *180*, 332.
(15) Morgan, P. E. D.; Carroll, P. J.; Lange, F. F. *Mater. Res. Bull.* **1977**, *12*, 251.
(16) Borisov, S. V.; Klevcova, R. F. *J. Struct. Chem.* **1963**, *4*, 575.
(17) Warren, B. E. *X-Ray Diffraction*; Addison Wesley Publishing: Reading, MA, 1969; pp 47–49.
(18) Peters, C. R., manuscript in preparation.
(19) Fukushima, E.; Roeder, S. B. W. *Experimental Pulse NMR*; Addison-Wesley: London, 1981.
(20) Carduner, K. R. *J. Magn. Reson.* **1989**, *81*, 312.

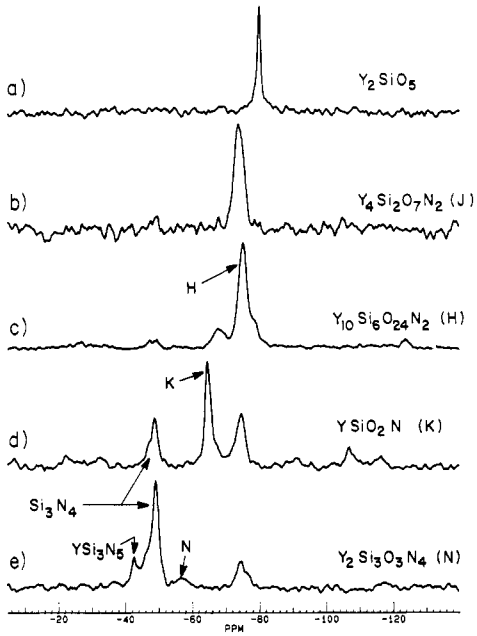

Figure 1. Silicon-29 MAS NMR (59.5 MHz) spectra of Y–Si–O–N phases prepared for reference materials. Each spectrum represents 24 acquisitions with a 1-h delay. Most samples were not pure. The components of interest in each sample are labeled by their chemical formula and a letter.

spectrum, as with the ^{29}Si data, by using standard Fourier transform and phasing routines. Spectra are referenced to $Al(H_2O)_6Cl_3$ whose resonance is established at 0 ppm. Downfield resonances are at positive values of the parts per million scale.

Ceramic samples were prepared for MAS NMR by machining pieces into cylinders for insertion into alumina or zirconia rotors. For Bruker MAS rotors, the dimensions of the cylinders (not the same as rotor volume) are 0.216 ± 0.001 in. wide by 0.470 ± 0.001 in. long. The cylinders easily slide into the rotors with slight play (if they are too tight they cannot be removed from the rotor). Despite the loose fit, the cylinders come up to the speed of the rotor, as indicated by the sideband displacement. Cylinders of sintered Si_3N_4 were generally easy to spin. On the other hand, cylinders made from the Y–Si–O–N samples could not be spun faster than 500 Hz. This problem is attributed to the existence of voids in the unsintered materials. Double air bearing rotors are often very sensitive to lack of symmetry of samples and may not spin if the sample cannot achieve a uniform distribution in the rotor (as is possible using powders). For this reason, the Y–Si–O–N samples were all run as powders. These materials are easily powdered in any type of impact grinder or miniball mill. Other issues related to preparation of ceramic for MAS NMR analysis are presented elsewhere.[21]

Results

Y–Si–N–O Phases. Dupree et al.[10] present a comprehensive NMR study of these phases giving both the resonance positions and an interpretive comparison of the spectra with results from powder X-ray diffraction. Their work shows that the chemical shift of ^{29}Si is dependent on the number of oxygens and nitrogens tetrahedrally bonded to the silicon. This dependence is well resolved in the MAS NMR spectrum, and thus they were able to choose among alternative structures for some of these phases that had not been resolved by previous powder X-ray diffraction work. In the following, the results of their work as well as our own results are employed for spectra assignments. The similarity between our spectra and those given by Dupree et al.[10] lends confidence to the validity of the assignments. The ^{29}Si MAS NMR spectra of a series of five samples of these phases are given in Figure 1. Only the spectra of Y_2SiO_5 and $Y_4Si_2O_7N_2$, Figure 1a,b respectively, show pure materials. All of the other samples consist of mixtures of the phases. The resonance frequencies and line widths are collected in Table I along with corresponding data from Dupree et al.[10] obtained at a 20% higher field strength (71.535 MHz vs 59.631 MHz). If the line width were exclusively a result of dispersion of the chemical shift due to partial amorphous character, then one would expect line widths of Dupree et al. to be somewhat wider than those from our work (on the hertz scale). This prediction does appear to be the case, with some exceptions. Since the preparation conditions are not known to be exactly the same for the two studies, the comparison of line widths cannot be strictly valid and will require further work. One could, for example, obtain spectra from the same samples at different fields to see how the line widths change. The reader is referred to Dupree et al.[10] for a complete discussion of the significance of the resonance positions with respect to crystal structures of the Y–Si–O–N phases.

Table I. Spectral Parameters for Processed Si_3N_4 Ceramic[a]

phase	peak maxima, ppm	fwhh, Hz
β-SiN_4		
sintered	−48.5	116
precursor	−48.7[b]	150[b]
α-Si_3N_4		
sintered	−47.1	
	−49.5	
precursor	−46.8[b]	
	−48.9[b]	
	Y–Si–O–N Phases	
$Y_{10}Si_6O_{24}N_2$	−74.9	190
	−67.4	250
	−74.8[c]	210[c]
	−67.5[c]	250[c]
$Y_4Si_2O_7N_2$	−73.7	240
	−74.4[c]	320[c]
$YSiO_2N$	−64.7	139
	−65.3[c]	400
$Y_2Si_3O_4N_4$	−57.1	270
	−56.7[c]	430[c]
YSi_3N_5	−42.8	
	−45.5[c]	140[c]
	−42.3[c]	
Y_2SiO_5	−80.0	76
	−79.8[c]	80[c]

[a] Error on values if ±2 of the last significant figure quoted. [b] From: Carduner, K. R.; Carter III, R. O.; Milberg, M. E.; Crosbie, G. M. *Anal. Chem.* **1987**, *59*, 2797. [c] ±30 Hz. From: Dupree, R.; Lewis, M. H.; Smith, M. E. *J. Am. Chem. Soc.* **1988**, *110*, 1083.

Sintered Silicon Nitride. The sintering of Si_3N_4 results in the conversion of α powder to β needles to form an interlocking structure. The densification of α to β is aided by the formation of an intergranular phase made up of the Y–Si–O–N compounds. These compounds, resulting from the reaction of Y_2O_3 with Si_3N_4, are molten during sintering. The reaction products remain in the final ceramic material and are reflected in the ^{29}Si MAS NMR spectra of samples of sintered Si_3N_4 ceramics. The effect of sintering on the spectrum of Si_3N_4 is illustrated in Figure 2, which shows, in part a, UBE-10 Si_3N_4 powder and two samples of sintered ceramic, test ceramic 1 in part b ("repeat of D" in ref 12), and test ceramic 2 in part c ("A" in ref 12). The difference in signal-to-noise in the spectrum depicted in Figure 2a when compared to the two spectra of sintered ceramic is due to the increase in sample density by the sintering process. There are more ^{29}Si atoms in the

(21) Rokosz, M. J.; Carduner, K. R.; Carter III, R. O. *J. Magn. Reson.*, submitted.

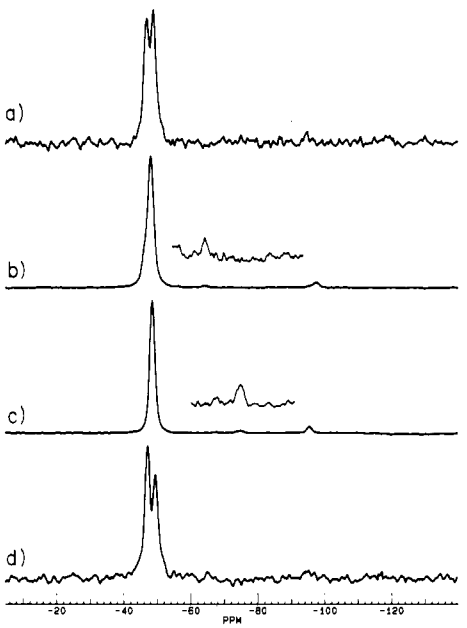

Figure 2. Silicon-29 MAS NMR spectra of (a) UBE E-10 (lot no. A-22, α-Si_3N_4 powder), (b) test ceramic 1, (c) test ceramic 2, and (d) residual spectrum from 1 after subtraction of scaled version of 2. Each spectrum represents 24 acquisitions with a 1-h delay. The vertical expansions are by a factor of 10.

Table II. Weight Percentages of Second Phases, Primary Components, and Densities of Test Ceramics

	Y–Si–N–O phase[a]		Si_3N_4		density	
ceramic	H	K	α	β	immersion	NMR[b]
1		4.7 (14.4)	30.5	64.8	3.173	3.3
2	12.2 (12.9)			87.8	2.846	2.9

[a] Theoretical weight percent in parentheses assuming all yttria is converted to this phase. [b] $Density_{NMR} = (wt_{UBU\text{-}10}/vol_{rotor}) \times (int_{ceramic}/int_{UBE\text{-}10})$.

sample volume after sintering. In fact, by integrating the spectra of the powder for comparison against the integrated signal of the ceramics, a measure of the increase in density of the ceramic may be obtained. Results of this procedure are given in the last two columns of Table II, which compare density as determined by immersion[12] and by the NMR integrals. It can be seen that the agreement is quite satisfactory. As a side note, these data show that it is possible for a ceramic showing less α to β conversion than another sample to have a higher sintered density. The explanation for this effect, discussed at length in ref 12, relates to the sintering program, specifically to the heating rate, which was faster for ceramic 1. The importance of fast heating rate to the densification of Si_3N_4 is discussed in ref 12. Moreover, it was found that hold time above 1700 °C was most important for the α to β conversion. This was shorter for ceramic 1 than for ceramic 2.[12]

Consistent with the expected conversion of α to β material during sintering, the similarity of the spectrum of ceramic 2 (Figure 2c) to that for the β powder[1] is not surprising. The line width in the ceramic is narrowed from 150 Hz for the powder to 116 Hz for the ceramic (see Table I). The narrowing of the line width reflects a reduction of microscopic disorder, which is expected to be greater in the powder.[22] For ceramic 1 (Figure 2b), a shoulder is just visible on the low-field side of the principal peak.

(22) Hatfield, G. R.; Carduner, K. R. *J. Mater. Sci.*, in press.

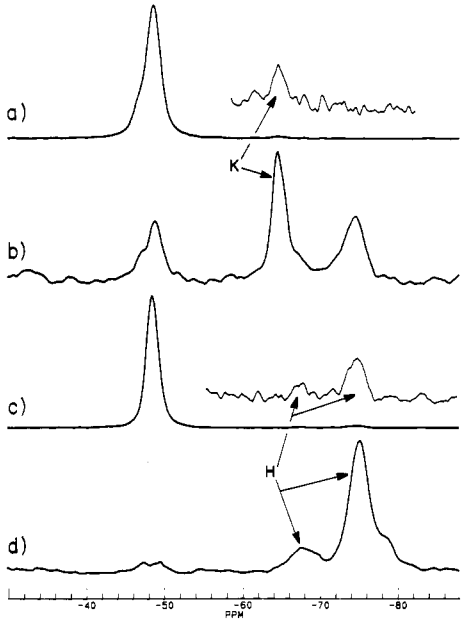

Figure 3. Silicon-29 MAS NMR spectra of (a) test ceramic 1 (horizontal expansion of by a factor of 10), (b) $YSiO_2N$ phase, (c) test ceramic 2, and (d) $Y_5Si_3O_{12}N$ phases.

Table III. Composition of Sintered Si_3N_4–Y_2O_3–Al_2O_3 Mixtures: Comparison of NMR Spectroscopy and Powder X-ray Diffraction Results

	MAS NMR (X-ray)			
sample	H	K	α	β
1[a]	0 (3.6)	4.7 (6.5)	30.5 (14.1)	64.8 (75.4)
2[b]	12.2 (10.7)	0 (0)	0 (0)	87.8 (89.3)
3[c]	0 (4.7)	0 (5.9)	34.0 (19.7)	66.0 (69.7)
4[d]	0 (7.1)	2.5 (2.3)	0 (0)	97.5 (90.6)
5[e]	0 (7.9)	5 (0.1)	10.5 (4.1)	84.5 (87.9)

[a] "Repeat of D" in ref 11. [b] Run A. [c] Run D. [d] Run B. [e] Run C.

If the spectrum for ceramic 2 is scaled and subtracted from that for 1, the residual spectrum, shown in Figure 2d, represents the α component from Si_3N_4 powder that did not convert during sintering. Integration of the spectrum for 1 before and after subtraction gives the α/β ratio of the sintered ceramic sample. For 1, this ratio is $^1/_2$. For the set of five ceramic samples, prepared according to the sintering cycle program variations described in ref 12, the α/β ratio derived in this manner was found to range from 0 to 0.8.

The intergranular Y–Si–O–N compounds produce less intense features, when they appear, in the ^{29}Si MAS NMR spectrum. If sufficient signal averaging is performed, these resonances can be observed above the noise and integrated for comparison against the more predominant line from the Si_3N_4. Typical spectra of intergranular phases are shown by the vertically expanded traces in Figure 2b,c and in Figure 3a,c for test ceramics 1 and 2, respectively. In Figure 3b,d, the spectra for two of the Y–Si–O–N samples are reproduced. The phase in the ceramic was identified by the correspondence of its resonance with that from the respective Y–Si–O–N sample. Integration of the peak from the intergranular phase and from the major Si_3N_4 peak allows for determination of the weight percent of the grain boundary phase when the relative formula weights are taken into consideration.[22] The results of this procedure for these samples are given in Tables II and III for the other samples investigated. The comparison with the X-ray data is discussed below.

Chemistry of Alumina in the Sintered Ceramics. Alumina-27 recently has been applied to study structure

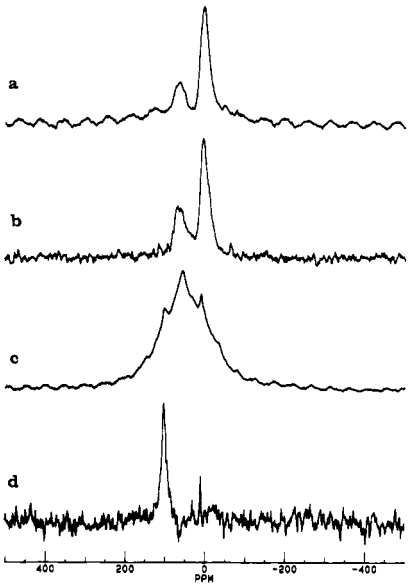

Figure 4. Aluminum-27 MAS NMR spectra of (a) commercially available γ-alumina (50 acquisitions, 1-s delay, 2.5-μs 90° pulse), (b) same using TOSS (512 acquisitions, TOSS sequence and timing described in ref 13), (c) ceramic 1 (1 000 000 acquisitions, 200-ms recycle delay), and (d) same using TOSS (300 000 acquisitions).

in a variety of ceramic materials,[23] especially aluminas[24,25] and sialons,[26,27] and has been advanced beyond its well-known use to study structure and chemistry in zeolite catalysts.[28] Techniques to acquire MAS NMR spectra of ^{27}Al have recently been discussed.[20] Given the wealth of background material on solid-state ^{27}Al NMR chemical shifts, it became apparent that acquisition of the weak ^{27}Al spectrum from the sintered Si_3N_4 ceramics might result in an interpretable spectrum. The results of the application of ^{27}Al MAS NMR are illustrated in Figure 4a,b for γ-alumina, where Figure 4b was acquired by using the TOSS sequence discussed in ref 20, which removes sidebands from both the central and satellite transitions. Likewise, Figure 4c,d shows the spectrum from ceramic 1. Acquisition conditions are presented in the caption. γ-Alumina contains aluminum atoms in both octahedral and tetrahedral coordinations, as indicated by the appearance of two peaks in the ^{27}Al MAS NMR spectrum (at 66 and 5 ppm, respectively). When applied to ^{27}Al, TOSS will tend to discriminate against components of the sample that have short T_1 because of the relatively long time period required for the TOSS pulse sequence. The effect explains why the TOSS spectrum of the ceramic, Figure 4d, has only a single peak at 105 ppm; the other two peaks have been selectively removed. A comparison with the data presented by Dupree et al.[27] indicates this resonance to come from the β'-sialon Si_5AlON_7, which only has one type of Al environment and thus one peak in its ^{27}Al MAS NMR spectrum. Contrasting behavior is illustrated in Figure 5a,b, the single pulse and TOSS spectrum of another β'-sialon $SiAl_2O_2N_2$, which has three types of Al sites and thus three lines in its spectrum. Since all of these sites should have similar T_1's, each site contributes

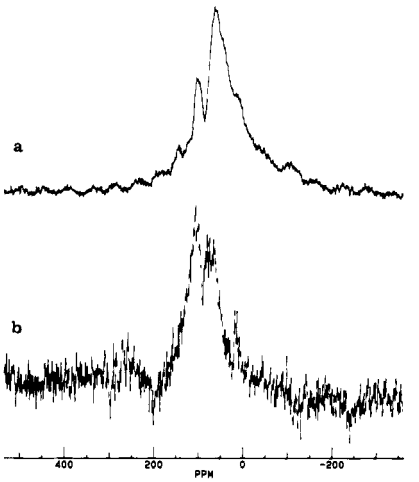

Figure 5. Aluminum-27 MAS NMR spectra of β'-sialon ($SiAl_2O_2N_2$, sample courtesy of M. E. Smith) by using (a) a single 90° pulse (10 000 acquisitions, 0.5-s recycle delay) and (b) TOSS (100 000 acquisitions, 0.5-s recycle delay, TOSS sequence was ca. 500 μs long).

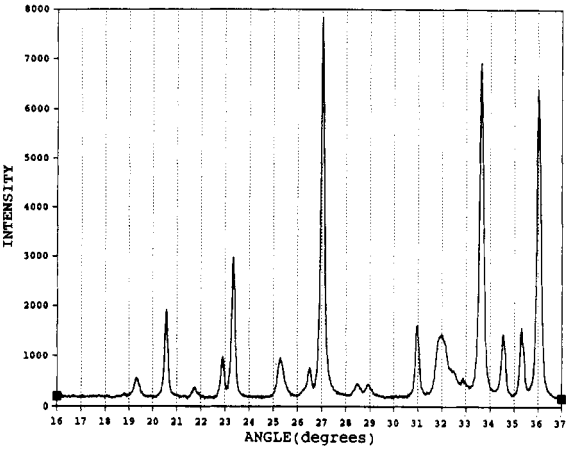

Figure 6. Observed X-ray powder diffraction spectrum for NMR cylinder 3 (see Table III). Features for both the H and K Y–Si–O–N phases are observable.

to the TOSS spectrum. In the ceramic samples, the missing intensity in the TOSS spectrum may indicate that there is residual alumina following sintering (although it is unlikely that this remains as γ-alumina given the sintering temperature) and that this component has shortened T_1. One possibility is that this residual alumina resides at grain boundary phases that are rich in paramagnetic impurity, which is known to be present in these samples.[29]

Comparison of Composition Results from NMR Spectroscopy and X-ray Diffraction. The compositions of five different ceramic samples as determined by the NMR and X-ray techniques are given in Table III. A typical powder X-ray diffraction pattern is illustrated in Figure 6. Assignments of the features in this diffraction spectrum along with complete details on the fitting routine are provided in ref 18. Some of the X-ray analyses were repeated to gauge precision of the technique. These repeats showed less than ±0.5% variation in the weight percentage of any of the reported results. In other instances, larger variations for a given sample were observed when the analysis was performed on different pieces of the same ceramic. This was taken as evidence of macroscopic inhomogeneity in the sample. These differences were usually under 1% for the secondary phases and under 10%

(23) Akitt, J. W. *Prog. NMR Spectrosc.* **1989**, *21*, 1.
(24) Muller, D.; Gessner, W.; Behrens, H.-J.; Scheler, G. *Chem. Phys. Lett.* **1981**, *79*, 59.
(25) McMillan, M.; Brinen, J. S.; Haller, G. L. *J. Catal.* **1986**, *97*, 243.
(26) Klinowski, J.; Thomas, J. M.; Thompson, D. P.; Korgul, P.; Jack, K. H. *Polyhedron* **1984**, *3*, 1267.
(27) Dupree, R.; Lewis, M. H.; Smith, M. E. *J. Appl. Crystallogr.* **1988**, *21*, 109.
(28) Fyfe, C. A.; Thomas, J. M.; Klinowski, J.; Gobbi, G. C. *Angew. Chem.* **1983**, *22*, 259.

(29) Shinozaki, S., private communication.

for the crystalline Si_3N_4 phases when measured on a crushed sample. If the X-ray analysis was conducted at a given point on an uncrushed sample, then substantially greater compositional variation was observed. Generally speaking, the agreement between the two techniques shows mixed results, being quite good for sample **2** to less than satisfactory as regards the H and K phases for samples **3** and **5**. Overall, the agreement on the α and β phases composition is acceptable. Of note in the interpretation of this comparison of techniques is each of the ceramic samples showed approximately 5% amorphous Si_3N_4 (as determined by using the NMR procedure discussed in ref 1). Also, some of the line widths of the H and K phase peaks, when they were observed, tended to vary, indicating that these too had partially amorphous character. It may be concluded that insensitivity of the X-ray technique to the presence of amorphous phases coupled with the loss of signal for the NMR method due to the varying amounts of paramagnetic impurities in these samples is likely to be at the heart of the observed discrepancies between the two techniques. Paramagnetic impurities have been observed by thermal electron microscopy at the grain boundaries of the β microcrystals[29] and thus should disproportionately quench the H and K phases signals. This would explain the differences in measured composition for samples **3** and **4**. For sample **5**, where a K phase signal was observed and not seen by the X-ray, it should be noted that the K phase peak was somewhat wider that usual in this sample and thus the phase was probably partially amorphous. Alternatively, since the H phase signal was not observed at all in sample **5**, it is also possible that the presence of paramagnetic impurities, which completely removed the H phase peak, broadened the peak from the K phase.

Discussion

The combination of an ample delay between pulses and high-density, monolithic samples of sintered ceramic is sufficient to allow the identification and quantitation of the grain boundary phases produced by sintering aids used to assist in the conversion of α powder to β-Si_3N_4 ceramic components. While a number of workers have alluded to the necessity for long delays when acquiring spectra of Si-based ceramics, no one appears to be using the delay lengths used here. In the absence of any known methods for reducing the T_1's, delays of at least 1 h appear to be the only way to get quantitatively accurate spectra. Since it appears that a sufficient time delay had been inserted between pulses, it cannot be assumed that the low value for the concentration of K phase in ceramic **1** compared to the theoretical value (see Table II) is related to differences in T_1. In addition, the X-ray results also indicated lower K phase than theoretical. Rather, it may be that these samples still contain yttria or some other yttrium compound that does not contain silicon. Still another possibility is that the yttria is removed during the sintering process. Yttrium-89 MAS NMR experiments are planned to address this issue.[30]

Many studies over the past decade have shown the sensitivity of ^{29}Si MAS NMR to subtle solid-state chemistries.[31,32] Often, this chemistry has important effects on the physical properties of the materials under study. For yttria-doped Si_3N_4 ceramics, the subtle differences in composition of the intergranular phases have strong effects on the physical properties of the ceramic and thus techniques to nondestructively quantify these phases are important. Silicon-29 may provide an important tool for detecting solid-state chemistry in Si-based ceramics not easily studied by other techniques. Areas of its most significant potential contribution have been addressed in this report and in previous work.[1] These include quantitation of amorphous phases or regions and the ability to observe phases at low concentration. Given the impact of grain boundary phases on the physical properties of Si_3N_4 ceramic samples, the significance of a reliable technique to monitor these phases in controlling process related chemistry cannot be understated.

Conclusion

Silicon-29 MAS NMR has been used to study the grain boundary phases that result during sintering of Si_3N_4 powders in the presence of yttria added as a sintering aid. While these phases have been studied by themselves, this represents the first instance to our knowledge where they have been observed by NMR spectroscopy in a sintered ceramic. A series of five Si_3N_4 ceramic cylinders have been examined. The conversion from α to β-Si_3N_4 has been clearly observed and α/β ratios have been determined where less than complete conversion occurred. The comparison to the composition as determined by quantitative powder X-ray diffraction indicates separate areas of applicability for these techniques. The NMR spectrum is negatively influenced by the presence of paramagnetic impurities, which do not affect the X-ray spectra, while the NMR spectrum appears better when significant quantities of amorphous phases are present. It is safe to conclude that for the most accurate determination of composition, a multiple methodology approach is best.[33]

Acknowledgment. We thank J. M. Nicholson of Ford Research for providing ceramic samples. A portion of the support for this work (G.M.C. and E.D.S.) was provided by the U.S. Department of Energy, Office of Transportation Systems, Advanced Materials Program through the Ceramic Technology for Advanced Heat Engines Program at Oak Ridge National Laboratory, Oak Ridge, TN, under Contract DE-AC05-84OR21400 with Martin Marietta Energy Systems, Inc. H. D. Blair provided the samples of the Y–Si–O–N phases. M. E. Smith of the University of Warwick provided samples of β-Sialon. We also acknowledge the editor and reviewers for obvious care and insightfulness in their critical review.

Registry No. Si_3N_4, 12033-89-5; Y_2O_3, 1314-36-9; Al_2O_3, 1344-28-1; Y_2SiO_5, 12027-88-2; $Y_4Si_2N_2O_7$, 58694-26-1; $Y_{10}Si_6N_2O_{24}$, 59977-54-7; $YSiNO_2$, 62361-78-8; $Y_2Si_3N_4O_3$, 54650-98-5; YSi_3N_5, 112068-60-7.

(30) Dupree, R.; Smith, M. E. *Chem. Phys. Lett.* **1988**, *148*, 41.

(31) Fyfe, C. A. *Solid State NMR for Chemists*; C.F.C. Press: Ontario, 1983.

(32) Turner, G. L.; Kirkpatrick, R. J.; Risbud, S. H.; Oldfield, E. *Am. Ceram. Soc. Bull.* **1987**, *66*, 656.

(33) Mark, H.; Norris, K.; Williams, P. C. *Anal. Chem.* **1989**, *61*, 398.